



Published in final edited form as:

*Clin Pharmacokinet.* 2014 April ; 53(4): 361–371. doi:10.1007/s40262-013-0122-1.

## Integrated Population Pharmacokinetic/Viral Dynamic Modeling of Lopinavir/Ritonavir in HIV-1 Treatment Naïve Patients

Kun Wang<sup>1,2,3</sup>, David Z. D'Argenio<sup>2</sup>, Edward P. Acosta<sup>3</sup>, Anandi N. Sheth<sup>4</sup>, Cecile Delille<sup>4</sup>, Jeffrey L. Lennox<sup>4</sup>, Corena Kerstner-Wood<sup>3</sup>, and Ighovwerha Ofotokun<sup>4,\*</sup>

<sup>1</sup>Center for Drug Clinical Research, Shanghai University of Traditional Chinese Medicine, Shanghai, China.

<sup>2</sup>Biomedical Simulations Resource, University of Southern California, Los Angeles, California, USA.

<sup>3</sup>Division of Clinical Pharmacology, University of Alabama at Birmingham School of Medicine, Birmingham, Alabama, USA.

<sup>4</sup>Division of Infectious Disease, Department of Medicine, Emory University School of Medicine, Atlanta, Georgia, USA.

### Abstract

**Background**—Lopinavir (LPV)/ritonavir (RTV) co-formulation (LPV/RTV) is a widely used protease inhibitor (PI) based regimen to treat HIV-infection. As with all PIs, the trough concentration ( $C_{\text{trough}}$ ) is a primary determinant of response, but the optimum exposure remains poorly defined. The primary objective was to develop an integrated LPV population pharmacokinetic model to investigate the influence of  $\alpha$ -1-acid glycoprotein (AAG) and link total and free LPV exposure to pharmacodynamic changes in HIV-1 RNA and assess viral dynamic and drug efficacy parameters.

**Methods**—Data from 35 treatment-naïve HIV-infected patients initiating therapy with LPV/RTV 400/100 mg orally twice daily across two studies were used for model development and simulations using ADAPT. Total LPV ( $LPV_t$ ) and RTV concentrations were measured by high-performance liquid chromatography (HPLC) with ultraviolet (UV) detection. Free LPV ( $LPV_f$ ) concentrations were measured using equilibrium dialysis and mass spectrometry.

**Results**— $LPV_t$  typical value of clearance ( $CL_{LPV_t/F}$ ) was 4.73 L/h and distribution volume ( $V_{LPV_t/F}$ ) was 55.7 L. Clearance ( $CL_{LPV_f/F}$ ) and distribution volume ( $V_f/F$ ) for  $LPV_f$  were 596 L/h and 6370 L, respectively. Virion clearance rate was  $0.0350 \text{ h}^{-1}$ . Simulated  $LPV_{LPV_t} C_{\text{trough}}$  at 90% ( $EC_{90}$ ) and 95% ( $EC_{95}$ ) maximum response were 316 and 726 ng/mL, respectively.

**Conclusion**—The pharmacokinetic/pharmacodynamic model provides a useful tool to quantitatively describe the relationship between LPV/RTV exposure and viral response. This comprehensive modeling and simulation approach could be used as a surrogate assessment of ARV where adequate early phase dose-ranging studies are lacking in order to define target trough concentrations and possibly refine dosing recommendations.

\*Correspondence Ighovwerha Ofotokun, M.D., MSc. Associate Professor Division of Infectious Disease, Department of Medicine Emory University School of Medicine 49 Jesse Hill Jr. Drive, Atlanta, GA 30303 Phone: 404-616-0659; Fax: 404-616-0592; iofotok@emory.edu.

#### Conflicts of Interest:

All authors declare no conflicts or interest

## 1. Introduction

Over the past several years, it has become evident that achieving and maintaining adequate antiretroviral (ARV) concentrations is required to produce a sustained virologic response. It is also well recognized that the durability of an ARV regimen is limited not only by inadequate drug exposure and subsequent development of viral resistance, but also by the occurrence of toxicities often related to long-term exposure to higher plasma and tissue drug concentrations [1].

Protease inhibitors (PIs) are bound with high affinity primarily to  $\alpha$ -1-acid glycoprotein (AAG), thus free plasma concentrations are inversely related to AAG concentrations. As an acute phase protein, AAG synthesis rises significantly in response to acute and chronic inflammation such as encountered with infections and injuries [2], a factor that may account for the observed variability in plasma AAG concentrations with chronic HIV-infection. Given the PIs high binding affinity for AAG, their high plasma concentrations in the presence of ritonavir (RTV), and the low saturation capacity of AAG, it has been speculated that variations in AAG levels could result in clinically important changes in PI pharmacokinetics and pharmacodynamics. Since a free drug's concentration more accurately reflect its availability to target cells, changes in AAG concentrations could have important clinical implications. However, the inverse relationship between free drug and binding protein concentrations is likely an over simplification of their dynamics. Under normal physiologic conditions, plasma protein binding has little or no effect on the free concentrations for many drugs. This is because at steady state, equilibrium is maintained between free drug concentrations and plasma drug clearance such that the elimination rate is increased as free concentrations increase, and vice versa[3]. For certain drugs, alterations in protein binding can lead to clinically significant changes in pharmacokinetics and pharmacodynamics [4].

Lopinavir (LPV) is an inhibitor of the HIV-1 protease. LPV, co-formulated with low dose ritonavir (RTV) [Kaletra (LPV/RTV, 400/100 mg)], is a frequently used PI regimen for the treatment of HIV infection because of its high effectiveness and reasonable tolerability. LPV is primarily metabolized by cytochrome P450 3A4 (CYP3A4), but co-administration with low dose RTV, a potent inhibitor of CYP3A4, significantly increases LPV plasma concentrations [5]. The *in vitro* half maximal inhibitory concentration ( $IC_{50}$ ) of LPV is approximately 10-fold lower than that of RTV, and RTV systemic exposure is low following a 100 mg dose [6]. Thus the antiviral activity of LPV/RTV is due primarily to LPV [6, 7]. A mechanistic understanding of the complex interplay between free concentrations, CYP3A4 inhibition, plasma protein binding, antiviral efficacy and development of viral resistance will lead to more informed dosing strategies with currently approved ARVs and those in development.

Establishing ARV concentrations that exceed the susceptibility of the virus is required for robust suppression of viral replication. PI trough concentrations ( $C_{trough}$ ) are correlated with response, but determination of target  $C_{trough}$  values are hindered by a dearth of *in vivo* concentration-response data typically determined during early phase drug development. Without *in vivo* concentration-response data, protein binding adjusted *in vitro* susceptibility measurements may provide surrogate estimates for the optimal *in vivo*  $C_{trough}$ . To date, population models directly linking free PI concentrations to drug response *in vivo* are lacking. To address this limitation, we developed an integrated population model to describe the influence of AAG on the equilibrium of total and free plasma LPV concentrations, including the effect of RTV exposure and other relevant covariates. The integrated model also links free LPV concentrations to HIV-1 viral dynamics, which allows an assessment of

the role of clinically relevant changes in LPV binding on changes in plasma viral load in treatment naïve HIV-infected individuals with predominantly wild-type virus.

## 2. Subjects and Methods

### 2.1 Subjects and Study Design

Data from two studies in treatment-naïve HIV-infected patients initiating ARV therapy were used for these analyses. Both studies were conducted at a single center, and were prospective, multiple dose intensive single and/or steady state pharmacokinetic studies in which subjects were recruited from the Grady Infectious Diseases program (IDP) out-patient clinic in Atlanta, Georgia, USA. Eligibility included male and female subjects age 18 years and HIV-1 RNA PCR > 50,000 copies/mL. Subjects were not enrolled if they were on medications that could interact with the PIs, on investigational ARV agents, had active opportunistic infection, had renal/hepatic impairment, or were pregnant. At enrollment, demographic information and clinical laboratory data were collected, and ARV adherence counseling was provided to all subjects. Subjects initiated therapy with LPV/RTV 400/100 mg orally twice daily plus standard dosing of 2 nucleoside reverse transcriptase inhibitors. All subjects provided written informed consent before undergoing any study procedures. These trials were designed according to the ethical guidelines for human studies and approved by the Emory University Institutional Review Board.

Plasma AAG concentrations were quantified using an enzyme-linked immunosorbent assay (ELISA). Total LPV (LPV<sub>t</sub>) and RTV were measured by high-performance liquid chromatography (HPLC) with ultraviolet (UV) detection [8]. Free LPV (LPV<sub>f</sub>) was quantitated using equilibrium dialysis followed by mass spectrometry. A reversed-phase high performance liquid chromatographic (HPLC) assay, coupled to a triple quadrupole mass spectrometer (MS/MS) for detection, was developed and validated for the determination of free LPV in human plasma (range of 0.25 to 80 ng/mL). Sample preparation involved equilibrium dialysis, the addition of a labeled isotope internal standard (Lopinavir d-8, IS), and a simple protein precipitation method using acetonitrile. The sample was dried down and reconstituted in 100 µL of 50/50 acetonitrile/water to concentrate the sample. Reversed phase chromatographic separation of LPV and IS was performed on an Atlantis® dC18 2.1 × 100 mm column under isocratic conditions. A binary mobile phase was used consisting of 20% 0.1% formic acid in water and 80% 0.1% formic acid in acetonitrile. The detection and quantitation was achieved for LPV and IS by multiple reaction monitoring (MRM). The de-protonated molecular ions [M-H]<sup>-</sup> were monitored at m/z 629.5 → 447.1 for LPV, and 637.5 → 447.2 for IS. These provided adequate sensitivity with minimal interference from endogenous matrix components.

In study 1 (S1), 16 patients underwent intensive plasma sampling (1, 2, 3, 4, 6, 8, 10 and 12 hr post dose) at 2 and 16 weeks post treatment initiation. The study population, design and enrollment criteria have been previously reported [9]. In study 2 (S2), 20 patients underwent plasma sampling (-2, 0, 1, 2, 3, 4 hr) on day 1 (second dose) and at weeks 2 and 24. In S2, intensive HIV-1 RNA sampling was also performed. Pre-dose (time 0) AAG and HIV-1 RNA samples were obtained and the first dose of a LPV/RTV-based ARV regimen was administered during a 48-hour clinic visit. All S2 participants also received tenofovir disoproxil fumarate and emtricitabine. Intensive HIV-1 RNA samples were collected at hours 2, 4, 6, 12, 18, 24, 30, 36, 42, and 48, and days 3, 4, and 7. Additional HIV-1 RNA samples were collected at weeks 2, 3, 4, 8, 12, 16, 20, and 24. CD4 T-cell counts were obtained at baseline and weeks 8, 16, and 24 as per standard of care. Follow-up AAG and pharmacokinetic samples were collected at weeks 2 and 24.

Thirty six subjects from both studies were available for population pharmacokinetic analysis, and 20 of the S2 subjects had intensive HIV-1 RNA sampling. Thirty five subjects were used for pharmacokinetic analysis: one subject with very low LPV concentrations (suggesting poor adherence) was excluded. Nineteen subjects from S2 were used for pharmacokinetic/pharmacodynamic analyses. One subject with 10 viral load measurements above the limit of quantitation was removed. Five viral load measurements from three different subjects were excluded due to likely problems with adherence.

## 2.2 Mathematical Modeling

The population model was developed sequentially by first creating a joint model for LPV<sub>t</sub> and RTV, followed by an independent model relating AAG and LPV<sub>t</sub> with LPV<sub>f</sub>. A viral dynamic model was then developed simultaneously with CD4 cell count results and integrated with the submodels to construct the composite final Pharmacokinetic/Pharmacodynamic model depicted in Figure 1. As indicated in Figure 1, LPV<sub>t</sub> CL<sub>LPV<sub>t</sub>/F</sub> depends on the concentration of ritonavir (C<sub>RTV</sub>), where LPV<sub>f</sub> concentration (C<sub>LPV<sub>f</sub></sub>) is a function of both LPV<sub>t</sub> (C<sub>LPV<sub>t</sub></sub>) and AAG. The LPV effect on viral dynamics was modeled by linking C<sub>LPV<sub>f</sub></sub> through transit delay compartments.

Population analysis was used to develop each of the four components of the overall pharmacokinetic/pharmacodynamic model. Maximum likelihood estimates for model parameters were obtained through the application of the expectation maximization algorithm to the parametric, nonlinear mixed-effects maximum likelihood model, as proposed and developed by Schumitzky [10] and Walker [11] and implemented in ADAPT (version 5, MLEM module) [12]. Model parameters were assumed to follow a multivariate log-normal distribution, with stage 1 random error taken to be normally distributed with a proportional plus additive error variance.

The following covariates collected at baseline were evaluated for their ability to explain the interindividual variability (IIV) in base model parameters: sex, age, race, weight, height, BMI (body mass index), serum creatinine, creatinine clearance, and hepatic enzymes aspartate aminotransferase (AST) and alanine aminotransferase (ALT). The criterion for a covariate to be added to the final model was a decrease of more than 3.84 in minus two loglikelihood value (-2LL), which corresponds to a P value of 0.05 (log likelihood ratio test). Finally, a stepwise backward elimination was carried out. The criteria for a covariate to remain in the final model was P<0.01, corresponding to a decrease of 6.63 in the -2LL.

Model evaluation was assessed using prediction corrected visual predictive check (pcVPC) [13] with NONMEM (version VII), Perl speaks NONMEM (PsN, version 3.4.2) [14], and Xpose (version 4.4.0) [15] (1000 data sets were simulated). The 95% confidence interval of the median, 5th and 95th percentile of the simulated concentrations at different times were calculated and compared with the prediction corrected observations.

**2.2.1 Pharmacokinetic Models**—Data from S1 and S2 were used for population modeling of LPV<sub>t</sub> and RTV. Initially, separate models for LPV<sub>t</sub> and RTV were established by considering one and two compartment models with and without an absorption lag phase (model selection based on the likelihood ratio test). Next, a joint model of LPV<sub>t</sub> and RTV (LPV<sub>t</sub>/RTV) was developed using LPV<sub>t</sub> and RTV measurements simultaneously by examining various models to represent the relationship between RTV concentrations and LPV<sub>t</sub> clearance [16]. The following equations (1-4) represent the joint model for both drugs, including an exponential term for the effect of RTV concentration on LPV<sub>t</sub> clearance:

$$\frac{d}{dt}A1 = - \frac{CL_{LPVt0} \cdot \exp[-c_1 \cdot (C_{RTV} - 299)]}{V_t} \cdot A1 + k_{aLPVt} \cdot A2 \quad (1)$$

$$\frac{d}{dt}A2 = - k_{aLPVt} \cdot A2 \quad (2)$$

$$\frac{d}{dt}A3 = - \frac{CL_{RTV}}{V_{RTV}} \cdot A3 + k_{aRTV} \cdot A4 \quad (3)$$

$$\frac{d}{dt}A4 = - k_{aRTV} \cdot A4 \quad (4)$$

In the above equations, A1 and A2 are the amount of LPV<sub>t</sub> in the measured (central) and absorption compartments, respectively, while A3 and A4 represent the amounts of RTV in the measured and absorption compartments, respectively (all amounts in mg). In Eq. (1), CL<sub>LPVt0</sub> (L/h) is the typical LPV<sub>t</sub> clearance and is used to explain the effect of RTV (C<sub>RTV</sub>, which equals A3/V<sub>RTV</sub> in mg/L) on LPV<sub>t</sub> clearance.

The value 299 in Eq. 1 is the median RTV concentration and C<sub>1</sub> is the RTV effect coefficient. CL<sub>RTV</sub> (L/h) is the clearance of RTV, while V<sub>LPVt</sub> (L) and V<sub>RTV</sub> (L) are the distribution volumes of LPV<sub>t</sub> and RTV, and k<sub>aLPVt</sub> (h<sup>-1</sup>) and k<sub>aRTV</sub> (h<sup>-1</sup>) are the LPV<sub>t</sub> and RTV absorption rate constants. Throughout the model, CL and V terms represent apparent clearance and volume (CL/F and V/F) for LPV<sub>t</sub> and RTV as well as LPV<sub>f</sub>.

**2.2.2 AAG - Dependent LPV<sub>f</sub> Model**—The model relating both LPV<sub>f</sub> and LPV<sub>t</sub> to AAG assumes that LPV<sub>f</sub> is in rapid equilibrium with LPV<sub>t</sub>. A separate population analysis relating measured LPV<sub>t</sub> and AAG concentrations (model inputs) to LPV<sub>f</sub> concentrations (observations) was conducted using the pooled data from S1 and S2, and the following model was selected based on previously reported data[17]:

$$C_{LPVf} = [fu_0 - p_1 \cdot (AAG - 91.8)] \cdot C_{LPVt} \quad (5)$$

where *fu*<sub>0</sub> is the fraction of unbound LPV at the median AAG (91.8 mg/dL) and *p*<sub>1</sub> is the slope for AAG.

**2.2.3 HIV-1 Viral Dynamic Model**—To describe the measured plasma HIV-1 RNA concentrations and the CD4+ T-cell counts obtained in S2, we adopted, with slight modification, the following previously reported model [18, 19], representing HIV and immune system dynamics during antiviral treatment.

$$\frac{d}{dt}T = \lambda - dT - \beta TV \quad (6)$$

$$\frac{d}{dt}I = \beta Tv - \delta I \quad (7)$$

$$\frac{d}{dt}v = N\delta \cdot (1 - \varepsilon)I - cv \quad (8)$$

These three differential equations represent target CD4+ T-cells (T, cells/ $\mu$ L), infected CD4+ T-cells (I, cells/ $\mu$ L) and free virions (v, copies/mL). The measured CD4 count data is the combined total of states T and I. The parameter  $\lambda$  (mL/h) is the rate of formation new CD4+ T-cells,  $d$  ( $h^{-1}$ ) is the death rate of CD4+ T-cells,  $\beta$  (mL/h/virion) is the infection rate,  $\delta$  ( $h^{-1}$ ) is the death rate of infected CD4+ T-cells,  $c$  ( $h^{-1}$ ) is the clearance rate of free virions,  $N$  (particles/h) is the number of new virions produced by each infected CD4+ T-cell during its lifetime, and  $\varepsilon$  represents the concentration of free drug required to inhibit viral replication (efficacy). To account for the delay between the initiation of therapy and the observed decrease in viral load, mainly attributed to the time required for the completion of the viral replication cycle in productively infected cells [20], several transit delay compartments were used to link  $C_{LPV_f}$  to the efficacy term  $\varepsilon$ . The transduction delay model is as follows:

$$\frac{d}{dt}D1 = \frac{1}{\tau} \left( \frac{I_{max} \cdot C_{LPV_f}^\gamma}{IC_{50}^\gamma + C_{LPV_f}^\gamma} - D1 \right) \quad (9)$$

$$\frac{d}{dt}D2 = \frac{1}{\tau} (D1 - D2) \quad (10)$$

$$\frac{d}{dt}\varepsilon = \frac{1}{\tau} (D2 - \varepsilon) \quad (11)$$

where D1 and D2 are the signals in the delay compartments,  $I_{max}$  is the maximum inhibition effect of LPV<sub>f</sub> (fixed at 1 assuming no escaping virus routes),  $IC_{50}$  is the concentration at half  $I_{max}$ ,  $\gamma$  is the hill coefficient, ( $h$ ) is the mean transit time for each compartment, and  $C_{LPV_f}$  is the predicted LPV<sub>f</sub> concentration. The latter was determined for each patient via a separate population analysis (one compartment model with lag time) using measured LPV<sub>f</sub> concentrations. For model building, 2, 3 and 4 transit delay compartments were evaluated. It was assumed that only LPV, not RTV, acts on the virus since the *in vitro* antiviral  $IC_{50}$  of LPV is approximately 10-fold lower than that of ritonavir [6]. It was further assumed that the viral dynamics are at steady state prior to the initiation of therapy, at least relative to the time course of drug action, and therefore the following relationships can be derived from Eqs. (6-8)

$$N = \frac{cv_0}{I_0\delta} \quad \beta = \frac{\delta I_0}{v_0 T_0} \quad \lambda = dT_0 + \delta I_0 \quad (12)$$

where  $T_0$ ,  $I_0$  and  $v_0$  are the initial value of target CD4+ T-cells, infected CD4+ T-cells, and viral load, respectively.

### 2.3 Exposure-Response Simulations

Simulation studies were conducted to explore exposure-response relationships using the LPV<sub>f</sub>, the AAG-dependent LPV<sub>f</sub>, and the viral dynamic models. Simulated LPV doses ranged from 5 mg to 700 mg twice daily (18 different doses). The pharmacodynamic determinant of response was the decrease in  $\log_{10}$  time averaged area under the viral load-time curve from 0 to 7 days ( $AUC_{0-7days}$ ) minus baseline (AAUCMB) [21, 22] of HIV-1 RNA. The AAUCMB was determined for each patient using their estimated population

mean values of viral dynamic model and AAUCMB was used to determine the average viral load decrease over the first 7 days of treatment. The goal of these simulations was to link the LPV<sub>f</sub> 12 hour steady-state concentrations (C<sub>f12h</sub>) to changes in AAUCMB and determine the corresponding LPV<sub>t</sub> 12 hour steady state concentration (C<sub>t12h</sub>) required to produce 50% (EC<sub>50</sub>), 90% (EC<sub>90</sub>), and 95% (EC<sub>95</sub>) of the maximum drug effect (E<sub>max</sub>). The exposure-response relationship of C<sub>f12h</sub> and decrease in AAUCMB was fitted using the following E<sub>max</sub> model:

$$\text{Decrease in AAUCMB} = \frac{E_{max} \cdot C_{f12h}^{hill}}{EC_{50}^{hill} + C_{f12h}^{hill}} \quad (13)$$

where E<sub>max</sub> is the maximum response, EC<sub>50</sub> is C<sub>f12h</sub> that corresponds to 50% of E<sub>max</sub>, and *hill* describes the shape of the sigmoid curve. The C<sub>f12h</sub> EC<sub>90</sub> and EC<sub>95</sub> values were calculated from Eq. (13) using the estimated values of EC<sub>50</sub> and *hill*. The corresponding EC<sub>95</sub> for C<sub>t12h</sub> was calculated using the AAG-dependent LPV<sub>f</sub> model (eq. (5)), for the median and range of C<sub>f12h</sub> and AAG measurements in this study.

### 3. Results

#### 3.1 Demographic and Baseline Data

Of the 35 subjects included in the pharmacokinetic modeling analysis, 25 were male and 10 were female, 31 were African American and 4 were Caucasian. Table 1 lists baseline values for several clinical variables. A total of 1218, 1236, 575 and 165 samples of RTV, LPV<sub>t</sub>, LPV<sub>f</sub> and AAG respectively, were collected and used for the pharmacokinetic analysis. In S2, a total of 412 measurements of HIV-1 RNA and 63 measurements of CD4 T-cell counts from 19 subjects were used for modeling. Changes in plasma HIV-1 RNA over time are shown in Supplementary Fig. 1.

#### 3.2 Mathematic Models

**3.2.1 Pharmacokinetic Models**—LPV<sub>t</sub> and RTV plasma concentrations were each well described by a one-compartment model with an absorption lag. A proportional model was used to describe the residual error variance. For the LPV<sub>t</sub> base model the population mean (IIV CV%) of clearance (CL<sub>LPV<sub>t</sub></sub>/F), volume (V<sub>LPV<sub>t</sub></sub>/F), absorption rate constant (k<sub>aLPV<sub>t</sub></sub>) and lag time (T<sub>lag,t</sub>) were 4.45 (34.6) L/h, 52.2 (54.9) L, 0.358 (77.7) h<sup>-1</sup> and 0.826 (59.8) h, respectively.

The combined LPV<sub>f</sub>/RTV model was constructed sequentially (the RTV model was established and its parameters fixed at their conditional mean estimates for each subject to develop the combined model) and includes BMI as a significant covariate (reduction of 9.81 in -2LL) explaining some of the variability in CL<sub>LPV<sub>t</sub></sub> as follows:

$$CL_{LPV_{t0}} = CL_{LPV_{t1}} \cdot e^{CL_{LPV_{t2}} \cdot (BMI - 22.5)} \quad (14)$$

where CL<sub>LPV<sub>t1</sub></sub> is typical clearance at median BMI (22.5 kg/m<sup>2</sup>) and CL<sub>LPV<sub>t2</sub></sub> is the coefficient of BMI effect. The population parameter estimates of the combined LPV<sub>f</sub>/RTV model are shown in Table 2 (BMI was not a significant covariate in the RTV analysis). The absorption rate constant (k<sub>aLPV<sub>t</sub></sub>) and lag time (T<sub>lag,t</sub>) for LPV<sub>t</sub> were both fixed to their individual conditional mean values from the separate LPV<sub>t</sub> modeling in developing the integrated LPV<sub>f</sub>/RTV model. An exponential term was used to incorporate the effect of RTV concentration on the clearance of LPV<sub>t</sub> (see Eq. (1)). At the median values of BMI (22.5 kg/m<sup>2</sup>) and plasma RTV concentration (299 ng/mL), the model predicts LPV<sub>t</sub> CL to be 4.73 (L/h). Figure 2 displays the individual prediction goodness of fit plots of LPV<sub>t</sub> and LPV<sub>f</sub>

concentrations for the combined LPV<sub>t</sub>/RTV model. The population prediction goodness of fit plots are presented in Supplementary Fig. 2. The prediction corrected visual predictive check (pcVPC) for LPV<sub>t</sub> and LPV<sub>f</sub> are shown in Figure 3, which represent the combination of week 2 and week 16 for S1, and week 2 and week 24 for S2.

**3.2.2 AAG-Dependent LPV<sub>f</sub> Model**—The LPV<sub>t</sub> and LPV<sub>f</sub> plasma concentration data from S1 and S2 were pooled, along with the associated AAG measurements, and a separate population analysis using Eq. (5) resulted in model parameter estimates shown in Table 2 (goodness of fit plots presented in Supplementary Fig. 3). Simulated *fu* as a function of AAG for each individual were also performed. The individual predictions over the AAG range measured in each subject are shown in Supplementary Fig. 4. The AAG-dependent LPV<sub>f</sub> model found that over the range of AAG values in the two studies (23.6 to 479 mg/dL) there is a significant effect of AAG on binding with *fu* values ranging from 0.00903 to 0.00389, which is consistent with prior protein-free LPV studies [23].

**3.2.3 HIV-1 Dynamic Model**—Table 2 lists the viral dynamic parameters derived using individual conditional mean values obtained from the LPV<sub>f</sub> and viral dynamic models from Eqs. (6-11). In this analysis, *d* and  $\delta$  could not be simultaneously estimated because CD4 cell count data was modeled using the combined total of states T and I. As a result, death rate of T cells (*d*) was fixed at reference value [24]. The resulting individual prediction goodness of fit plots for viral load and CD4 cell count are shown in Figure 4. Relative standard errors could not be calculated for the limited CD4+ cell results due to high variability. Despite this limitation, the viral load dynamic model described the time course of measured HIV-1 RNA data with reasonable fidelity, as indicated by the individual prediction plot (see Supplementary fig. 5). Moreover, estimated parameter values are generally comparable to those reported in several other studies as shown in Table 2. Results of the independent compartment model describing LPV<sub>f</sub> pharmacokinetics were used as parameter input for developing the HIV viral dynamic model presented in Table 3.

**3.2.4 Simulated Exposure-Response Model**—Based on the viral dynamic model simulation, the AAUCMB and C<sub>f12h</sub> with LPV dose ranging from 5 mg to 700 mg twice daily were obtained. The plot of decrease in AAUCMB vs. C<sub>f12h</sub> is shown in Figure 5 (a). A sigmoid E<sub>max</sub> model successfully described the decrease in AAUCMB relative to C<sub>f12h</sub> (exposure-response). The estimated E<sub>max</sub> was a decrease in the AAUCMB of 5.28 log<sub>10</sub> copies/mL, *hill* was 0.899, and the EC<sub>50</sub> for C<sub>f12h</sub> was 0.227 ng/mL. The calculated EC<sub>90</sub> and EC<sub>95</sub> for C<sub>f12h</sub> were 2.61 and 6.00 ng/mL, respectively. Figure 5 (b) depicts the decrease in AAUCMB vs. C<sub>t12h</sub>. The estimated EC<sub>50</sub>, EC<sub>90</sub>, and EC<sub>95</sub> for C<sub>t12h</sub> at the median (range) AAG concentration were 27.5 (25.1-58.3), 316 (289-672), and 726 (664-1542) ng/mL, respectively. The median LPV<sub>f</sub> and LPV<sub>t</sub> concentrations (interquartile range) at 12 hours post-dose at steady state were 368 (23.4-547) and 5327 (3870-8157) ng/mL, respectively.

## 4. Discussion

### 4.1 Pharmacokinetic Models

The population pharmacokinetic model parameter estimates for LPV<sub>t</sub> and RTV compared well with previously reported literature values. The estimated clearance of LPV<sub>t</sub> from the final model in this work is 4.73 L/h, compared to prior CL/F values ranging from 3.2 to 5.22 L/h [25-29]. Distribution volume for LPV<sub>t</sub> has been reported ranging from 42.6 to 61.6 L, [5, 25, 27] which is similar to our result of 55.7 L. The LPV<sub>t</sub> absorption rate (K<sub>a,LPV<sub>t</sub></sub>) shown in Table 2 is 0.325 h<sup>-1</sup>, which is also within the previously reported range of 0.267 to 0.564 h<sup>-1</sup> [5, 26]. While there have been no previously reported compartmental models for LPV<sub>f</sub>

pharmacokinetic on which to base a comparison of the results of our model presented in Table 2, several published studies have reported AUC values for LPV<sub>f</sub> following therapy with LPV/RTV. The estimated AUC<sub>0-12h</sub> obtained via simulation from our model is 414 ng-h/mL, while Boffito et al [30] reported an AUC<sub>0-12h</sub> result of 890.14 ng-h/mL, considerably higher than our result. However, this difference could be attributable to the different unbound fractions between the two studies: 0.92% vs. 0.73% (current studies). The differences in fraction unbound may itself be due to the differences in AAG ranges observed across patients in the two studies: 58–116 mg/dL vs. 23.6-479 mg/dL in the current studies. Of note, our studies enrolled treatment-naïve patients with advanced disease as evidenced by a baseline median CD4+ T-cell counts of 69 cells/μL. HIV-1 induced immune activation up-regulates AAG synthesis. Conversely, down regulation in immune activation following ARV therapy decreases AAG synthesis [2, 31]. Thus participants in our studies likely had higher baseline AAG concentrations due to their advanced disease and treatment-naïve status. Methodological differences may have also played a role in the different free AUC<sub>0-12h</sub> results, as our studies employed equilibrium dialysis compared with ultrafiltration.

#### 4.2 AAG-Dependent LPV<sub>f</sub> Model

An independent population analysis was performed to develop a model relating measured LPV<sub>t</sub> and AAG concentrations to LPV<sub>f</sub> concentrations (see Table 2 and Figure 4). A linear model (see Eq. (5)) best described the individual data over the AAG range of our studies. The data and modeling results presented herein suggest that variations in AAG concentrations could result in clinically significant changes in LPV pharmacokinetics. The model predicts that over the range of AAG values across the two studies there is a significant effect of AAG on LPV binding, with *fu* ranging from 0.00903 to 0.00389 (a 2.3 fold difference). Using the AAG-dependent LPV<sub>f</sub> model, the LPV<sub>f</sub> exposure changes can be predicted from AAG and C<sub>LPV<sub>t</sub></sub> measurements.

#### 4.3 HIV-1 Dynamic Model

In this work, we established a viral dynamic model to describe the viral load trajectory based on LPV<sub>f</sub> plasma concentration. This is the first analysis utilizing LPV<sub>f</sub> concentrations as the drug exposure metric linked to a HIV-1 viral dynamic model. The estimated drug efficiency and other viral dynamic parameters obtained in this study are in general agreement with other values reported in the literature as indicated in Table 2, with the exception of the death rate of infected CD4+ T-cells, which is smaller than the lowest value previously reported. The model estimated LPV<sub>f</sub> EC<sub>50</sub> is 5.84 ng/mL, which is consistent with the prescribing information for Kaletra from the US Food and Drug Administration[6] that indicates a range of LPV<sub>f</sub> concentrations of 3-7 ng/mL against several HIV-1 subtype B clinical isolates. In the presence of 50% human serum, the mean EC<sub>50</sub> of LPV against five laboratory strains ranged from 40-180 ng/mL.

#### 4.4 Simulated Exposure-Response Model

The median (interquartile range) of observed LPV C<sub>t12h</sub> at 400 mg (with 100 mg RTV) is 5327 (3870-8157) ng/mL. In contrast, the estimated C<sub>t12h</sub> required to achieve the EC<sub>95</sub> was 726 (664-1542) ng/mL at the median (range) AAG concentration in these two studies of 91.8 (23.6-479) mg/dL. Figure 5 depicts the simulated exposure-response relationship for LPV<sub>f</sub> (a) and LPV<sub>t</sub> (b). Despite the wide range of AAG results, the 25<sup>th</sup> percentile of observed C<sub>t12h</sub> (3870 ng/mL) was considerably greater than the modeled EC<sub>95</sub> of LPV<sub>f</sub>; even the 5<sup>th</sup> percentile of observed C<sub>t12h</sub> (1909 ng/mL) was 2.6 times greater than the EC<sub>95</sub> of LPV<sub>f</sub>. The simulated LPV<sub>t</sub> EC<sub>50</sub> was 27.5 ng/mL, which is lower than but relatively close to the range stated against different laboratory strains with 50% human serum and nearly

identical to the protein binding corrected EC50 (31 ng/mL) derived from a separate in vitro susceptibility study [32].

## 5. Conclusions and Clinical Implications

Collectively, these modeling and simulation results demonstrate in part why LPV/RTV is a highly effective PI treatment regimen. As seen in Figure 5, observed trough concentrations consistently exceed, by a large margin, the concentrations required to durably suppress HIV-1 replication *in vivo*. This creates some flexibility for patients receiving the drug, as deviations from a strict every 12 hour dosing schedule are unlikely to significantly affect clinically outcomes. Importantly, this modeling and simulation approach could serve as a surrogate for determining clinically significant target drug exposures that must be achieved and maintained for durable therapeutic success and to prevent drug resistant viral strains. Concentration-response relationships for many ARVs are scarce or non-existent. Our approach demonstrates that even for an ARV drug (particularly PIs) already approved for use at a fixed dose, it is possible to model and simulate minimum effective trough concentrations using data collected from well-designed clinical trials in a relatively small number of participants.

## Supplementary Material

Refer to Web version on PubMed Central for supplementary material.

## Acknowledgments

Supported by National Institutes of Health grants 1K23 A1073119 (IO), 5K12 RR017643 (IO), 1U01AI103408-01 (IO), P41-EB001978 (DZD), KL2TR000455 (ANS), UL1TR000454(ANS), Emory University CFAR (NIH P30 A1050409), and the Atlanta Clinical and Translational Science Institute (NIH MO1 RR00039). We would like to acknowledge the individuals that participated in these studies. Without their dedication this work could not have been accomplished.

## References

1. AIDSinfo. Guidelines for the use of antiretroviral agents in HIV-1-infected adults and adolescents. Department of Health and Human Services; 2013. Available at <http://aidsinfo.nih.gov/ContentFiles/AdultandAdolescentGL.pdf>. [6th July 2013]
2. Kushner I. The phenomenon of the acute phase response. *Annals of the New York Academy of Sciences*. 1982; 389:3–9-48.
3. Benet LZ, Hoener BA. Changes in plasma protein binding have little clinical relevance. *Clinical pharmacology and therapeutics*. Mar; 2002 71(3):1–15-21.
4. Belpaire FM, Bogaert MG. Pharmacokinetic and pharmacodynamic consequences of altered binding of drugs to alpha 1-acid glycoprotein. *Progress in clinical and biological research*. 1989; 300:3–37-50.
5. Crommentuyn KM, Kappelhoff BS, Mulder JW, et al. Population pharmacokinetics of lopinavir in combination with ritonavir in HIV-1-infected patients. *British journal of clinical pharmacology*. Oct; 2005 60(4):3–78-89.
6. FDA. [26th March 2013] prescribing information for KALETRA. Reference ID: 2909830. [cited; Available from: [www.accessdata.fda.gov/drugsatfda\\_docs/label/2011/021251s039,021906s032lbl.pdf](http://www.accessdata.fda.gov/drugsatfda_docs/label/2011/021251s039,021906s032lbl.pdf)]
7. Sham HL, Kempf DJ, Molla A, et al. ABT-378, a highly potent inhibitor of the human immunodeficiency virus protease. *Antimicrobial agents and chemotherapy*. Dec; 1998 42(12):3–218-24.
8. Ofotokun I, Chuck SK, Binongo JN, et al. Lopinavir/Ritonavir pharmacokinetic profile: impact of sex and other covariates following a change from twice-daily to once-daily therapy. *Journal of clinical pharmacology*. Aug; 2007 47(8):9–70-7.

9. Ofofokun I, Lennox JL, Eaton ME, et al. Immune activation mediated change in alpha-1-acid glycoprotein: impact on total and free lopinavir plasma exposure. *Journal of clinical pharmacology*. Nov; 2011 51(11):1–539-48.
10. Schumitzky, A. EM Algorithms and two stage methods in pharmacokinetic population analysis.. In: D'Argenio, DZ., editor. *Advanced methods of pharmacokinetic and pharmacodynamic systems analysis*. Vol. 2. Plenum Press; New York: 1995. p. 6-0.
11. Walker S. An EM Algorithm for Nonlinear Random Effects Models. *Biometrics*. 1996; 52(3):9–34-44.
12. D'Argenio, D.; Schumitzky, A.; Wang, X. ADAPT 5 user's guide: pharmacokinetic/ pharmacodynamic systems analysis software. *Biomedical Simulations Resource*; Los Angeles: 2009.
13. Bergstrand M, Hooker AC, Wallin JE, et al. Prediction-corrected visual predictive checks for diagnosing nonlinear mixed-effects models. *The AAPS journal*. Jun; 2011 13(2):1–43-51. [PubMed: 20967519]
14. Lindbom L, Ribbing J, Jonsson EN. Perl-speaks-NONMEM (PsN)--a Perl module for NONMEM related programming. *Computer methods and programs in biomedicine*. Aug; 2004 75(2):8–5-94.
15. Jonsson EN, Karlsson MO. Xpose--an S-PLUS based population pharmacokinetic/ pharmacodynamic model building aid for NONMEM. *Computer methods and programs in biomedicine*. Jan; 1999 58(1):5–1-64.
16. Zhang C, Denti P, Decloedt E, et al. Model-based approach to dose optimization of lopinavir/ ritonavir when co-administered with rifampicin. *British journal of clinical pharmacology*. May; 2012 73(5):7–58-67.
17. Baker SD, Li J, ten Tije AJ, et al. Relationship of systemic exposure to unbound docetaxel and neutropenia. *Clinical pharmacology and therapeutics*. Jan; 2005 77(1):4–3-53.
18. Wu H, Huang Y, Acosta EP, et al. Modeling long-term HIV dynamics and antiretroviral response: effects of drug potency, pharmacokinetics, adherence, and drug resistance. *Journal of acquired immune deficiency syndromes*. Jul 1; 2005 39(3):2–72-83.
19. Bonhoeffer S, May RM, Shaw GM, et al. Virus dynamics and drug therapy. *Proceedings of the National Academy of Sciences of the United States of America*. Jun 24; 1997 94(13):6–971-6.
20. Fang J, Jadhav PR. From in vitro EC50 to in vivo dose-response for antiretrovirals using an HIV disease model. Part I: a framework. *Journal of pharmacokinetics and pharmacodynamics*. Aug; 2012 39(4):3–57-68. [PubMed: 22219000]
21. Weller S, Radomski KM, Lou Y, et al. Population pharmacokinetics and pharmacodynamic modeling of abacavir (1592U89) from a dose-ranging, double-blind, randomized monotherapy trial with human immunodeficiency virus-infected subjects. *Antimicrobial agents and chemotherapy*. Aug; 2000 44(8):2–052-60.
22. Gieschke R, Fotteler B, Buss N, et al. Relationships between exposure to saquinavir monotherapy and antiviral response in HIV-positive patients. *Clinical pharmacokinetics*. Jul; 1999 37(1):7–5-86. [PubMed: 10491728]
23. Gulati A, Boudinot FD, Gerk PM. Binding of lopinavir to human alpha1-acid glycoprotein and serum albumin. *Drug metabolism and disposition: the biological fate of chemicals*. Aug; 2009 37(8):1–572-5. [PubMed: 18838503]
24. Funk GA, Fischer M, Joos B, et al. Quantification of in vivo replicative capacity of HIV-1 in different compartments of infected cells. *Journal of acquired immune deficiency syndromes*. Apr 15; 2001 26(5):3–97-404.
25. Takahashi M, Kudaka Y, Okumura N, et al. Pharmacokinetic parameters of lopinavir determined by moment analysis in Japanese HIV type 1-infected patients. *AIDS research and human retroviruses*. Jan; 2008 24(1):1–14-5. [PubMed: 18275341]
26. Dailly E, Reliquet V, Raffi F, et al. A population approach to study the influence of nevirapine administration on lopinavir pharmacokinetics in HIV-1 infected patients. *European journal of clinical pharmacology*. Apr; 2005 61(2):1–53-6. [PubMed: 15666173]
27. Bouillon-Pichault M, Jullien V, Azria E, et al. Population analysis of the pregnancy-related modifications in lopinavir pharmacokinetics and their possible consequences for dose adjustment. *The Journal of antimicrobial chemotherapy*. Jun; 2009 63(6):1–223-32. [PubMed: 18957393]

28. Ng J, Chiu YL, Awni W, et al. Pharmacokinetics and safety of the lopinavir/ritonavir tablet 500/125 mg twice daily coadministered with efavirenz in healthy adult participants. *Journal of clinical pharmacology*. Aug; 2012 52(8):1–248-54.
29. Overton ET, Tschampa JM, Klebert M, et al. The effect of acid reduction with a proton pump inhibitor on the pharmacokinetics of lopinavir or ritonavir in HIV-infected patients on lopinavir/ritonavir-based therapy. *Journal of clinical pharmacology*. Sep; 2010 50(9):1–050-5.
30. Boffito M, Hoggard PG, Lindup WE, et al. Lopinavir protein binding in vivo through the 12-hour dosing interval. *Therapeutic drug monitoring*. Feb; 2004 26(1):3–5-9. [PubMed: 14749542]
31. Bree F, Houin G, Barre J, et al. Pharmacokinetics of intravenously administered 125I-labelled human alpha 1-acid glycoprotein. *Clinical pharmacokinetics*. Jul-Aug;1986 11(4):3–36-42.
32. Acosta EP, Limoli KL, Trinh L, et al. Novel method to assess antiretroviral target trough concentrations using in vitro susceptibility data. *Antimicrobial agents and chemotherapy*. Nov; 2012 56(11):5–938-45.
33. Schipani A, Dickinson L, Boffito M, et al. Simultaneous population pharmacokinetic modelling of atazanavir and ritonavir in HIV-infected adults and assessment of different dose reduction strategies. *Journal of acquired immune deficiency syndromes*. Jan 1; 2013 62(1):6–0-6.
34. Lopez Aspiroz E, Santos Buelga D, Cabrera Figueroa S, et al. Population pharmacokinetics of lopinavir/ritonavir (Kaletra) in HIV-infected patients. *Therapeutic drug monitoring*. Oct; 2011 33(5):5–73-82.
35. Ho DD, Neumann AU, Perelson AS, et al. Rapid turnover of plasma virions and CD4 lymphocytes in HIV-1 infection. *Nature*. Jan 12; 1995 373(6510):1–23-6.
36. Mohri H, Bonhoeffer S, Monard S, et al. Rapid turnover of T lymphocytes in SIV-infected rhesus macaques. *Science*. Feb 20; 1998 279(5354):1–223-7.
37. Wei X, Ghosh SK, Taylor ME, et al. Viral dynamics in human immunodeficiency virus type 1 infection. *Nature*. Jan 12; 1995 373(6510):1–17-22.
38. Perelson AS, Neumann AU, Markowitz M, et al. HIV-1 dynamics in vivo: virion clearance rate, infected cell life-span, and viral generation time. *Science*. Mar 15; 1996 271(5255):1–582-6.
39. Dimitrov DS, Willey RL, Sato H, et al. Quantitation of human immunodeficiency virus type 1 infection kinetics. *Journal of virology*. Apr; 1993 67(4):2–182-90.
40. Stafford MA, Corey L, Cao Y, et al. Modeling plasma virus concentration during primary HIV infection. *Journal of theoretical biology*. Apr 7; 2000 203(3):2–85-301.

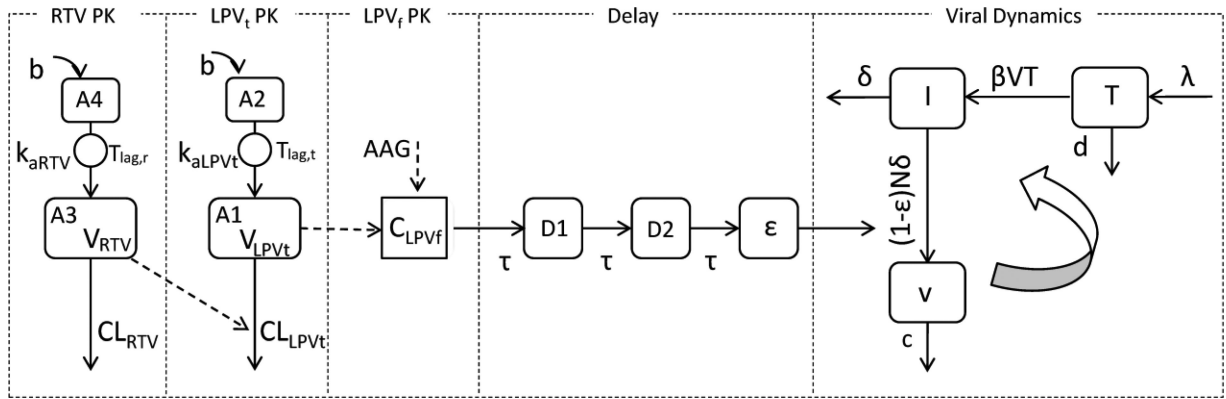


**Figure 1.**

Structure of the final integrated pharmacokinetic-pharmacodynamic model defined by Eqs. (1-11). (RTV: ritonavir;  $LPV_t$ : total lopinavir;  $LPV_f$ : free lopinavir; b: bolus input; A1: central compartment of LPVt; A2 depot compartment of LPVt; A3: central compartment of RTV; A4: depot compartment of ;  $CL_{LPVt}$ : Clearance of LPVt with ritonavir effect; RTV;  $CL_{RTV}$ : clearance of RTV;  $V_{RTV}$ : volume distribution of RTV central compartment;  $V_{LPVt}$ : volume distribution of LPVt central compartment;  $C_{LPVf}$ : concentration of LPVf;  $k_{aLPVt}$ : absorption rate constant of LPVt;  $k_{aRTV}$ : absorption rate constant of RTV;  $T_{lag,t}$ : absorption lag time of LPVt;  $T_{lag,r}$ : RTV absorption lag time; AAG:  $\alpha$ -1-acid glycoprotein;  $C_{LPVf}$ : free lopinavir concentration; D1 and D2: delay compartments. mean transit time; T: CD4+ T-cells; I: infected CD4+ T-cells; v free virions;  $\lambda$  the rate of new T cells are generated in the body; d the death rate of T cells;  $\beta$  the infection rate;  $\delta$  the death rate of infected CD4+ T-cells; c: the clearance rate of free virions; N: the number of new virions produced by each infected CD4+ T-cell during its lifetime;  $\epsilon$  the drug inhibit efficacy.

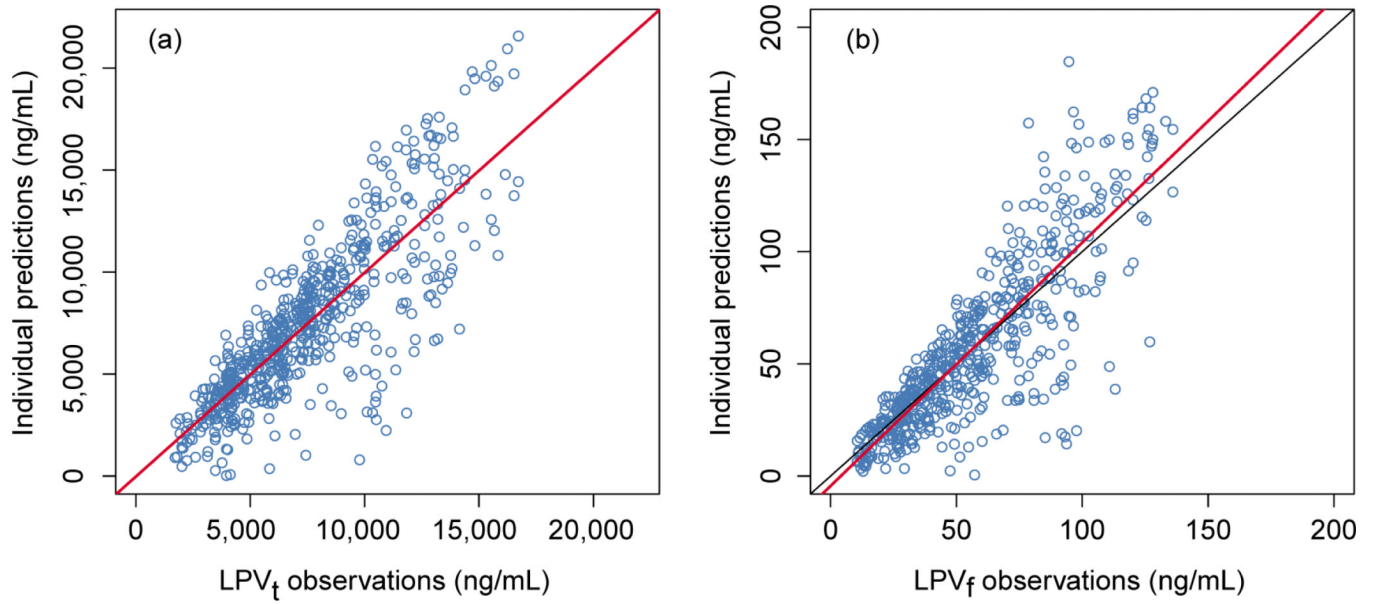


**Figure 2.**

The goodness of fit of individual predictions plots for the combined total lopinavir/ritonavir (LPV<sub>t</sub>/RTV) model (a) and the free lopinavir (LPV<sub>f</sub>) model (b). Symbols are the observed data; the red lines are the linear regression fit; the black lines are the lines of unity.

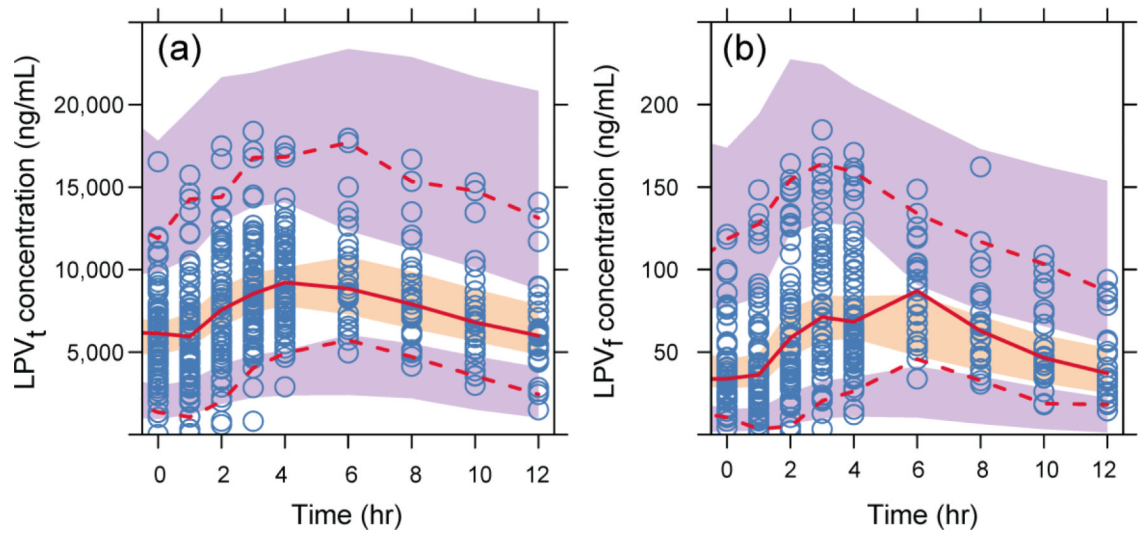


**Figure 3.** Prediction corrected visual predictive check of the combined total lopinavir/ritonavir (LPV<sub>t</sub>/RTV) model (a) and free lopinavir (LPV<sub>f</sub>) (b). The middle solid line is the median. The dash lines are the 5<sup>th</sup> and 95<sup>th</sup> percentiles of observed data. The shaded areas are the corresponding 95% confidence intervals of the simulated data.

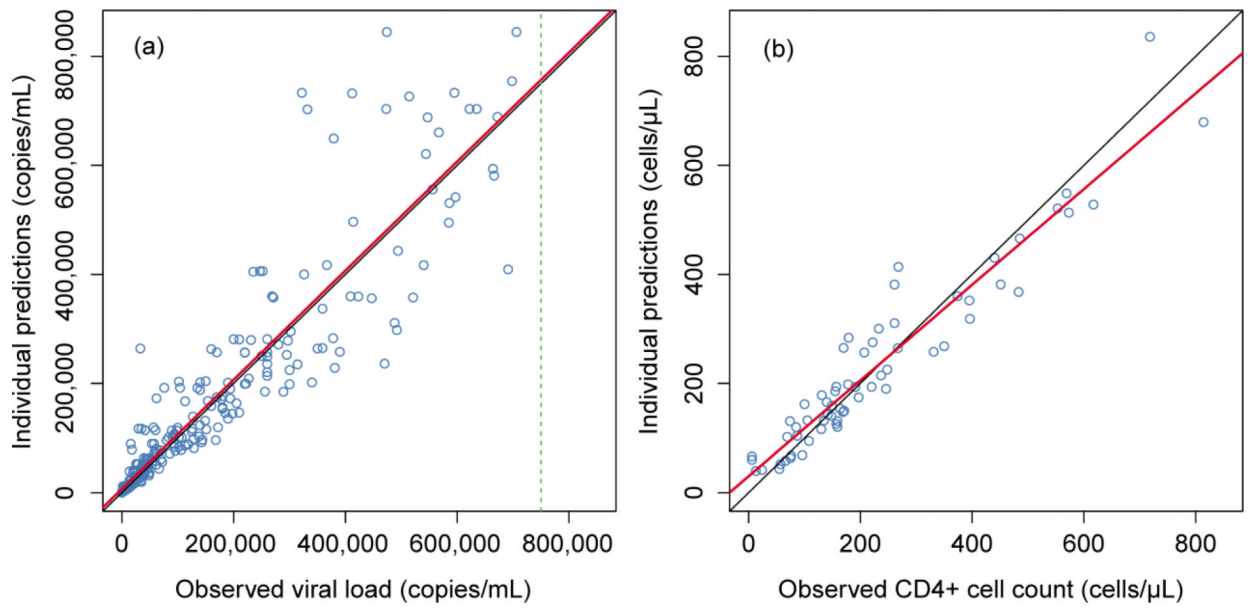


**Figure 4.**

Goodness of fit of individual predictions plots for viral load (a) and CD4 cell count (b). The symbols are the observed data; the red lines are the linear regression; the black lines are the line of unity; dashed line is the upper limit of HIV-1 RNA quantitation.

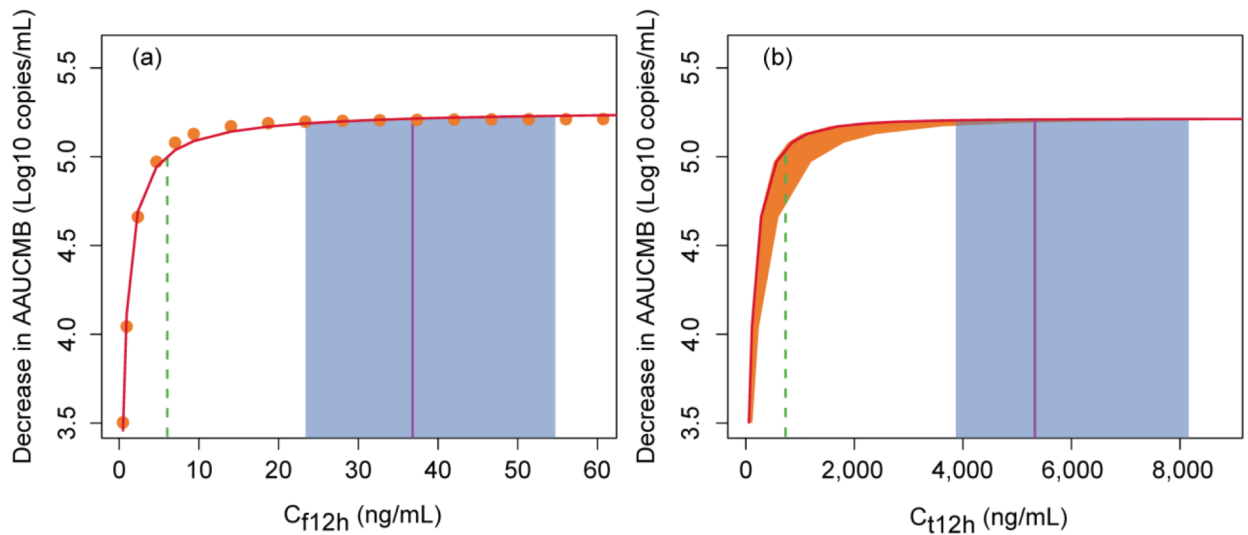


**Figure 5.**

Relationship between 12 hour steady-state concentrations of free lopinavir ( $C_{f12h}$ ) (a), total lopinavir ( $C_{t12h}$ ) (b) and exposure [expressed as decrease in area under the viral load-time curve minus baseline (AAUCMB)] at day 7. The symbols and the solid red curve in (a) are the predicted  $C_{f12h}$  and sigmoid  $E_{max}$  fitted line, respectively. The  $C_{t12h}$  was calculated by eq. (5) with  $C_{f12h}$  and  $\alpha$ -1-acid glycoprotein (AAG). The solid red curve and shaded orange area around the curve corresponds to the median (range) AAG of 91.8 (23.6-479) mg/dL in (b). The vertical dash green, solid purple line and shaded blue areas are the estimated  $EC_{95}$ , observed median and interquartile range of  $C_{f12h}$  and  $C_{t12h}$  at lopinavir/ritonavir 400/100 mg, respectively.

**Table 1**

## Baseline Demographics and Clinical Characteristics

Characteristics	Median (interquartile range)
Age (yr)	38.5 (33.8-47.3)
Weight (kg)	64.5 (59.6-74.3)
Body mass index (kg/m <sup>2</sup> )	22.5 (21.4-24.9)
Log <sub>10</sub> HIV-1 RNA PCR <sup>a</sup> (copies/mL)	5.18 (4.73-5.61)
Plasma α-1-acid glycoprotein (AAG) (mg/dL)	91.8 (67.4-134.)
Baseline CD4 + T-cell counts (cells/μl)	69.0 (20.5-153.)
Creatinine clearance <sup>b</sup> (mL/min)	99.3 (73.0-124.)
Aspartate amino transferase (mg/dL)	29.5 (24.0-52.6)
Alanine amino transferase (mg/dL)	30.5 (21.0-53.8)
Fraction of unbound lopinavir (%)	0.730 (0.540-0.953)

<sup>a</sup>PCR: polymerase chain reaction

<sup>b</sup>Creatinine clearance calculated by the Cockcroft-Gault equation.

Table 2

Population Estimation Results for the Final Combined Pharmacokinetic-Pharmacodynamic Model.

Parameter <sup>a</sup>	Mean (%RSE) <sup>e</sup>	IIV CV%(%RSE) <sup>e</sup>	Literature values	Reference
CL <sub>LPVt0</sub> (L/h)	--	24.0 (61.8)		
CL <sub>LPVt1</sub>	4.73 (14.6)	--	3.2-5.22	[25-29]
CL <sub>LPVt2</sub>	0.055 (34.5)	--	NA	
C <sub>1</sub>	6.24E-04 (47.5)	28.3 (259.)	NA	
V <sub>LPVt</sub> (L)	55.7 (15.2)	55.2 (30.7)	42.6-61.6	[5, 16, 25, 27]
K <sub>aLPVt</sub> (1/h) <sup>c</sup>	0.325	--	0.267-0.564	[5, 26, 27]
T <sub>lag,t</sub> (h) <sup>c</sup>	0.875 (32.7)	60.5 (63.2)	NA	
CL <sub>RTV</sub> (L/h)	22.0 (11.9)	50.5(18.3)	8.00-24.3	[16, 29, 33, 34]
V <sub>RTV</sub> (L)	177. (29.3)	61.7 (41.5)	81-275	[33, 34]
K <sub>aRTV</sub> (1/h)	0.740 (47.0)	107. (56.6)	0.898-1.57	[33, 34]
T <sub>lag,r</sub> (h)	1.10 <sup>d</sup> (52.3)	69.8(64.6)	1.05-1.96	[33, 34]
fu <sub>0</sub>	0.00930 (4.48)	23.4 (18.3)	NA	
p <sub>1</sub>	1.13E-05 (25.7)	103. (31.4)	NA	
c (1/h)	0.0350	39.3	0.0138 - 1.67	[24, 35]
IC <sub>50</sub> (ng/mL)	5.84	53.1	3-7	[6]
τ (h)	3.22	41.6	NA	
d (1/h)	2.5E-04 <sup>b</sup>	--	4.17E-05 - 4.17E-04	[24, 36]
Δ (1/h)	0.00288	61.6	0.00416 - 0.029	[24, 35, 37, 38]
γ	1.88	19.2	NA	
β (mL/h/virion)	4.79E-09	217.	8.3E-10 - 1.25E-8	[24]
γ (mL/h)	75.0	75.3	5.83 - 129	[24]
N (particles/h)	19.2	183.	4.17 - 292	[39, 40]

NA. Not available.

<sup>a</sup> LPVt: total lopinavir; RTV: ritonavir; CL<sub>LPVt0</sub>: LPVt clearance; CL<sub>LPVt1</sub>: typical clearance of LPVt with median BMI (body mass index); CL<sub>LPVt2</sub>: coefficient of BMI effect.; c<sub>1</sub>: the coefficient of RTV effect; V<sub>LPVt</sub>: distribution volume of LPVt; k<sub>aLPVt</sub>: absorption rate constant of LPVt; T<sub>lag,t</sub>: absorption lag time of LPVt; CL<sub>RTV</sub>: clearance of RTV; V<sub>RTV</sub>: RTV distribution volume; k<sub>aRTV</sub>: RTV absorption rate constant; T<sub>lag,r</sub>: RTV absorption lag time; fu<sub>0</sub>: fraction of unbound drug with median α-1-acid glycoprotein [AAG (91.8 mg/dL)] , and p<sub>1</sub> is slope for AAG; c: the clearance rate of free virions; I<sub>max</sub>: the maximum inhibition effect of free lopinavir (LPVf); IC<sub>50</sub>: LPVf concentration at half I<sub>max</sub>; τ mean transit time; d: the death rate of T cells; Δ death rate of infected CD4 cells; γ: hill coefficient; β infection rate; Δ: rate of new T cells are generated in the body; N: number of new virions produced by each infected CD4 cell during its lifetime.

<sup>b</sup> Fixed from reference [24].

<sup>c</sup> k<sub>aLPVt</sub> at and T<sub>lag,t</sub> obtained from LPVt model with BMI as a covariate.

<sup>d</sup> The maximum of T<sub>lag,r</sub> was limited to 1.5 hours.

<sup>e</sup> IIV: Inter-individual variability; CV: coefficient of variation; RSE: relative standard error.

**Table 3**Population Estimation Results for LPV<sub>f</sub> Model

Parameter <sup>a</sup>	Mean (%RSE) <sup>b</sup>	IIV CV% (%RSE) <sup>b</sup>
CL <sub>LPVf</sub> (L/h)	596. (9.61)	41.0 (17.2)
V <sub>LPVf</sub> (L)	6370 (15.9)	52.6 (26.3)
k <sub>al</sub> LPVf (1/h)	0.884 (47.5)	120. (95.6)
T <sub>lag,f</sub> (h)	1.05 (15.0)	45.1 (48.8)

<sup>a</sup>IIV: Inter-individual variability; CV: coefficient of variation; RSE: relative standard error.

<sup>b</sup>CL<sub>LPVf</sub>: free LPV (LPVf) clearance; V<sub>LPVf</sub>: LPVf distribution volume; k<sub>al</sub>LPVf: absorption rate constant; T<sub>lag,f</sub>: absorption lag time.